Pergamon

Bioorganic & Medicinal Chemistry 10 (2002) 1019–1024

BIOORGANIC & MEDICINAL CHEMISTRY

Molecular Structure and Stereoelectronic Properties of Herbicide Sulphonylureas

R. Galeazzi,[a,*] C. Marucchini,[b] M. Orena[a,*] and C. Zadra[b]

[a]*Dipartimento di Scienze dei Materiali e della Terra, Università di Ancona, Via Brecce Bianche, I-60131 Ancona, Italy*
[b]*Dipartimento Agroambientale e della Produzione Vegetale, Università di Perugia, Borgo XX Giugno 72, I-06121 Perugia, Italy*

Received 27 July 2001; accepted 5 October 2001

Abstract—MO theoretical calculations were used with the aim to investigate the electronic properties of a number of sulphonylureas **1**–**8** which are employed as antifeedants. Quantum chemical descriptors [electron density, molecular electrostatic potential (MEP), the topology of frontier orbitals and reactivity index] were determined for these compounds, aimed both to obtain a deeper insight in their mechanism of action and to correlate these properties with their activity as inhibitors of ALS synthase.

Introduction

Acetolactate synthase (ALS), a key enzyme in the branched-chain amino acid biosynthesis in bacteria, fungi and higher plants, constitutes a target for sulphonylurea herbicides which are the most active group of herbicidal compounds found to date.[1,2] They are unusual inhibitors in that they bear no obvious similarity to substrates nor allosteric effectors of this enzyme.[3,4]

Whereas a number of *Graminaceae* are eliminated by these weed killers, both wheat and barley are relatively tolerant and remain practically unaffected, owing to rapid metabolism of these compounds.[5–7] So far, structure-based approaches for site-directed mutagenesis of ALS have been precluded by the lack of a crystal structure of this enzyme. Since the 3D structure of acetolactate synthase and consequently the inhibition site of sulphonylureas are still unknown,[8,9] useful information may be obtained from the conformational and theoretical properties of a number of these compounds, in order to correlate the stereoelectronic properties with their intrinsic activity.[10–14]

Results and Discussion

Recently, heterocyclic sulphonamides, another class of herbicides, were found to interact with ALS through both the electron-poor portion of the sulphonamide bridge and the electron-rich region of the heterocyclic ring, their activity strongly depending upon electric charge translocation.[15]

Prompted by this report, the present investigation was carried out in order to elucidate both the structural and electronic properties responsible for the behaviour of sulphonylureas **1**–**8**, since the activity data for these compounds have already been reported in the literature.[16–18] Therefore, in order to build on a model for enzyme–substrate interaction, sulphonylureas **1**–**8** were examined (Scheme 1) and a complete scan of their conformational space was performed.[19] In this way, the most stable conformations lying in the range of 0.5 kcal/mol (the pharmacophoric conformations) were pointed out. Then, starting from the optimised structures, the following electronic quantum mechanical descriptors were calculated at AM1 level:[20–22]

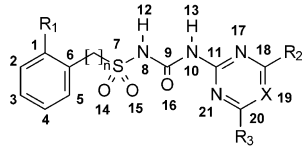

1. R_1 = COOMe, R_2 = R_3 = OMe, R_4 = H, Y = X = C, n = 1, Bensulfuron methyl
2. R_1 = COOMe, R_2 = R_3 = $OCHF_2$, R_4 = H, Y = X = C, n = 0, Primisulfuron
3. R_1 = COOMe, R_2 = Me, R_3 = OMe, R_4 = H, Y = C, X = N, n = 0, Metsulfuron meth
4. R_1 = OCH_2CH_2Cl, R_2 = Me, R_3 = OMe, R_4 = H, Y = C, X = N, n = 0, Triasulfuron
5. R_1 = COOEt, R_2 = Cl, R_3 = OMe, R_4 = H, Y = X = C, n = 0, Chlorimuron ethyl
6. R_1 = SO_2Et, R_2 = R_3 = OMe, R_4 = H, Y = N, X = C, n = 0, Rimsulfuron
7. R_1 = Cl, R_2 = Me, R_3 = OMe, R_4 = H, Y = C, X = N, n = 0, Chlorsulfuron
8. R_1 = COOMe, R_2 = R_3 = Me, R_4 = H, Y = X = C, n = 0, Sulfometuron methyl

Scheme 1.

*Corresponding author. Tel.: +39-071-220-4707; fax: +39-071-220-4714; e-mail: roberta@popcsi.unian.it

0968-0896/02/$ - see front matter
PII: S0968-0896(01)00357-1

1. Net atomic charges (Q_i)
2. HOMO and LUMO energies (ε_{HOMO}, ε_{LUMO}) and their 3D shapes
3. HOMO and LUMO orbital energy differences, $\Delta\varepsilon = \varepsilon_{LUMO} - \varepsilon_{HOMO}$ (energy gap)
4. Electrophilic frontier electron densities, $f_r^E = \Sigma_n [c_{(HOMO,n)}]^2$
5. Nucleophilic frontier electron densities, $f_r^N = \Sigma_n [c_{(LUMO,n)}]^2$
6. Indices of frontier electron density, $F_r^E = f_r^E/\varepsilon_{HOMO}$ and $F_r^N = f_r^N/\varepsilon_{LUMO}$
7. The reactivity index
8. The molecular electrostatic potential (MEP)

First, the charge distribution was considered, calculated according to the Mulliken Population Analysis,[23] an important chemical reactivity index and measurement of weak molecular interactions leading to electrostatic interactions. In this way, the most probable sites of hydrogen bond formation between the sulphonylurea herbicide and its target, the active site of ALS receptor, were identified. From Table 1, it can be seen that the partial positive charge is mainly located at S-7, whereas the negative ones lie at N-8, C-6, O-14 and O-15.

Subsequently, both the energy and topology of the frontier orbital were investigated, charge transfer interactions involving these orbitals being an important mode of ligand–receptor interactions. By considering the descriptors involved in the reactivity scale, the orbital energies for both HOMO and LUMO were calculated for all the significant conformations, and are reported in Table 2. The energy difference between the LUMO of an electron acceptor and the HOMO of an electron donor has long been used as a reactivity index.[24–27] In fact, according to the frontier molecular orbital theory (FMO) of reactivity, the formation of either a complex or a transition state relies upon an interaction between the frontier orbitals (HOMO and LUMO) of the reacting species. More recent investigations revealed that the HOMO–LUMO gap is an important stability index for the individual species concerned. A small difference between the HOMO and LUMO of a species is often due to a low lying LUMO and/or a high lying HOMO. On the contrary, a large HOMO–LUMO gap implies high stability and low reactivity in chemical reactions, and particularly low interaction with the target enzyme. The calculated values of $\Delta E_{HOMO-LUMO}$ reflect the scale of activity obtained from the experimental IC_{50} values.[16–18] In fact, **2**, **5** and **6**, which have the lowest energy gap, show the highest activity, whereas for Triasulfuron® **4** and Chlorsulfuron® **7**, where ΔE is higher, the corresponding activity is very low.

Table 1. Most significant atomic partial charges obtained from a Mulliken population analysis

Compound	C-6	N-8	O-14	O-15	S-7
1	−0.8186	−0.8385	−0.9004	−0.9155	2.8275
2	−0.7807	−0.8274	−0.9004	−0.9155	2.8548
3	−0.7630	−0.8467	−0.9163	−0.9244	2.8669
4	−0.8387	−0.8303	−0.9214	−0.9305	2.8882
5	−0.7724	−0.8752	−0.9035	−0.9448	2.8472
6[a]	−0.5612	−0.8806	−0.9038	−0.9245	2.8402
7	−0.8183	−0.8309	−0.9082	−0.8309	2.8553
8	−0.7738	−0.8306	−0.9178	−0.9063	2.8538

In Table 1 are reported the values for only one conformer of compounds **1**–**8**, since the other conformers showed no change.
[a]Significant values were obtained also for C-1 (−0.7562). C*R-1 (−0.8722), O-32*R1 (−0.9261), S*R1 (2.8441).

The HOMO–LUMO distribution for all compounds was then calculated (Table 3) and the 3D shapes were examined.[28,29]

The data obtained show that HOMO lies mainly on the heterocyclic ring, whereas LUMO is located on the sulphur atom and the aromatic ring bearing sulphur (Figs 1, 2). However, in Triasulfuron®, **4**, and Chlorsulfuron®, **7**, the HOMO lies on the aromatic ring bearing the sulphur atom, although its shape is very similar to other sulphonylureas. LUMO, on the other hand, maintains the same shape and location (Figs 3–5).

According to these findings, it would seem that HOMO distribution on the heterocyclic ring is essential for high herbicide activity. On the contrary, when HOMO and LUMO are located on the same side of the molecule, herbicidal activity strongly decreases, as it occurs for both Triasulfuron® **4** and Chlorsulfuron® **7**.

In addition, for sulphonylureas **1**–**8**, both relative and absolute electron frontier densities were calculated in order to characterise donor–acceptor interactions,[30,31] since most chemical reactions occur by maximum superimposition of HOMO and LUMO of the reagents. As a consequence, in a charge-transfer process, the electrophilic electron density is significant for the donor, whereas nucleophilic electron density is important for the acceptor (Table 3).

Table 2. HOMO, LUMO energies and heat of formation of the pharmacophoric conformations of sulphonylureas **1**–**8**

Compound	HOMO energy (eV)	LUMO energy (eV)	$\Delta E_{HOMO-LUMO}$ (eV)	ΔH_f (kcal/mol)
1	−9.31	−1.04	8.27	−173.17
	−9.56	−1.05	8.51	−173.18
	−9.38	−1.14	8.24	−172.86
	−9.59	−1.04	8.55	−172.97
	−9.39	−1.15	8.24	−172.80
2	−10.03	−1.31	8.72	−388.88
	−9.89	−1.45	8.44	−3.88.41
3	−10.15	−1.22	8.93	−118.22
	−10.16	−1.21	8.95	−118.21
	−10.39	−1.11	9.28	−117.80
4	−10.01	−0.98	9.03	−1.96
5	−9.68	−1.30	8.38	−138.08
6	−9.39	−1.64	7.75	−137.93
	−9.39	−1.64	7.75	−137.76
	−9.38	−1.64	7.74	−137.33
7	−10.02	−0.96	9.06	−44.26
	−10.09	−1.03	9.06	−44.09
	−10.08	−1.02	9.06	−44.09
8	−9.63	−0.97	8.66	−104.70
	−9.46	−0.98	8.48	−105.27
	−9.36	−0.95	8.41	−104.69

Table 3. (a) Indexes for electrophilic frontier electron density $[F_r^e\ (_{HOMO})]\times10^{-2}$

Compound	N-10	N-19	N-21	C-1	C-2	C-4	C-5	C-19
1(A)	−1.36	—	-2.49×10^{-3}	-2.75×10^{-5}	-1.58×10^{-6}	-2.05×10^{-5}	-8.71×10^{-5}	$-\times4.66$
1(B)	−1.48	—	−0.685	-9.32×10^{-5}	-4.03×10^{-5}	-2.43×10^{-5}	-8.20×10^{-5}	−4.43
1(C)	−1.28	—	−0.701	-1.11×10^{-4}	-8.0×10^{-6}	-4.55×10^{-5}	-4.05×10^{-5}	−4.66
1(D)	−1.50	—	−0.615	-2.90×10^{-4}	-1.37×10^{-4}	-8.65×10^{-5}	-3.02×10^{-4}	−4.41
1(E)	−1.27	—	-0.4×62	-1.16×10^{-4}	-1.41×10^{-4}	-5.07×10^{-5}	-3.95×10^{-5}	−4.65
2(A)	−1.75	—	-8.02×10^{-3}	-9.35×10^{-4}	-6.39×10^{-4}	-9.25×10^{-5}	-1.05×10^{-5}	−4.41
2(B)	−1.61	—	−0.822	-2.00×10^{-6}	-7.92×10^{-6}	-1.54×10^{-5}	-3.44×10^{-5}	−4.22
3(A)	−2.27	−2.29	−2.76	-1.29×10^{-4}	-1.82×10^{-3}	-9.54×10^{-5}	-1.64×10^{-4}	—
3(B)	−2.25	−2.75	−2.27	-1.15×10^{-4}	-6.24×10^{-5}	-6.48×10^{-5}	-1.12×10^{-4}	—
3(C)	−2.75	−2.49	−1.89	-2.48×10^{-2}	-6.18×10^{-2}	-2.23×10^{-2}	−0.187	—
4(A)	-1.27×10^{-3}	-1.88×10^{-4}	-1.97×10^{-4}	−2.05	−1.83	−2.72	−1.35	—
5(A)	−1.71	—	−1.27	-1.8×10^{-4}	-2.79×10^{-5}	-9.25×10^{-5}	-8.26×10^{-5}	−3.82
6(A)	−1.33	—	−0.575	-3.22×10^{-6}	-8.83×10^{-6}	-4.12×10^{-6}	-1.99×10^{-5}	−4.56
6(B)	−1.37	—	−0.635	-4.90×10^{-6}	-1.46×10^{-5}	-1.71×10^{-5}	-3.24×10^{-5}	−4.58
6(C)	−1.36	—	−0.585	-4.14×10^{-6}	-1.41×10^{-5}	-1.93×10^{-5}	-3.94×10^{-5}	−4.59
7(A)[a]	-9.90×10^{-5}	-3.46×10^{-5}	-3.15×10^{-5}	−2.17	−1.98	−2.58	−1.58	—
7(B)[b]	-7.17×10^{-5}	-1.78×10^{-5}	-6.46×10^{-5}	−2.16	−1.97	−2.56	−1.58	—
7(C)[c]	-7.86×10^{-5}	-2.94×10^{-5}	-9.55×10^{-5}	−2.16	−1.98	−2.56	−1.59	—
8(A)	−2.38	—	−9.81	-1.18×10^{-4}	-7.83×10^{-4}	-8.31×10^{-5}	-1.02×10^{-3}	−3.45
8(B)	−2.24	—	−8.59	-7.93×10^{-5}	-4.22×10^{-5}	-2.43×10^{-5}	-7.74×10^{-5}	−3.68
8(C)	−2.43	—	−9.51	-1.16×10^{-4}	-1.45×10^{-4}	-9.90×10^{-5}	-1.81×10^{-3}	−3.56

(b) Indexes for nucleophilic frontier electron density $[F_r^n\ (_{LUMO})]\times10^{-2}$

	S−7	O−14	O−15	C−1	C−2	C−3	C−4	C−5/N−5	C−6
1(A)	−37	−8.67	−8.80	−5.47	−0.716	−3.55	−3.62	−0.473	−6.05
1(B)	−36	−9.46	−8.26	−5.04	−0.395	−3.31	−3.42	−0.418	−5.69
1(C)	−36	−8.56	−8.70	−3.60	1.62×10^{-4}	−2.58	−2.13	−0.532	−3.93
1(D)	−36	−8.45	−8.98	−5.48	−0.358	−3.58	−3.61	−0.566	−6.08
1(E)	−36	−8.64	−8.78	−3.22	0.112	−2.43	−1.82	−0.581	−3.50
2(A)	−11	−0.123	−2.22	−13	-6.97×10^{-2}	−12	−5.61	−3.36	−14
2(B)	−15	−0.828	−2.94	−9	-2.81×10^{-2}	−10	−3.53	−11	−12
3(A)	−13	−2.17	−2.60	−14	-2.28×10^{-2}	−14	−6.57	−3.82	−16
3(B)	−11	−2.13	−1.89	−14	-7.45×10^{-2}	−14	−7.33	−3.59	−17
3(C)	−12	−2.72	−2.77	−15	-9.73×10^{-2}	−15	−7.75	−1.75	−17
4(A)	−24	−4.35	−5.41	−20	−1.61	−62	−2.54	−10.1	−16
5(A)	−12	−2.22	−2.51	−12	-2.88×10^{-3}	−13	−5.44	−4.13	−15
6(A)	−6.83	−1.40	−1.28	−13	−1.22	−7.87	−8.84	−0.62	−14
6(B)	−6.65	−1.38	−1.23	−13	−0.9	−7.87	−8.96	−0.616	−14
6(C)	−6.4	−1.29	−1.20	−11	−0.854	−7.99	−8.96	−0.546	−14
7(A)	−28	−5.47	−6.85	−10.36	−0.621	−13	−2.92	−5.66	−15
7(B)	−26	−6.62	−4.99	−9.51	−0.546	−13	−2.76	−5.72	−14
7(C)	−26	−5.16	−6.37	−9.59	−0.573	−13	−2.76	−5.88	−14
8(A)	−13	−2.38	−2.80	−18	-7.21×10^{-2}	−18	−9.38	−4.89	−21
8(B)	−11	−2.47	−2.68	−19	−0.147	−17	−10.3	−3.88	−22
8(C)	−15	−2.93	−3.13	−18	-1.41×10^{-2}	−18	−8.26	−5.24	−20

[a]R1-Cl,−1.44.
[b]R1-Cl,−1.42.
[c]R1-Cl,−1.41.

The results obtained point out that the highest LUMO density lies at S-7, together with some carbon atoms of the aromatic ring bearing the sulphur atom. On the contrary, HOMO has the maximum density at the ureic nitrogen and C-19 (or N-19) of the heterocyclic ring. On the other hand, Triasulfuron® **4** and Chlorsulfuron® **7** show a completely different pattern, the maximum density lying at C-1 and C-2, in agreement with the low IC_{50} values.

The reactivity of HOMO orbital at atom *i*, was established by using the $R_{(i)}$ index[32] which is correlated with the reactivity of sulphonylureas, as it is summarized in Tables 4 and 5. In fact, we observed that the highest indexes are generally observed for both ureic N-10 and X-19 and N-21 of the heterocyclic ring. On the contrary, in Triasulfuron® **4** and Chlorsulfuron® **7**, which show low IC_{50} values, the highest values refer to the ring bearing the sulphur atom.

Lastly, MEP was considered, which represents the electrostatic forces displayed by a ligand when it interacts with its receptor.[33,34] Three-dimensional MEP plots were calculated and the negative equipotential surfaces describe attractive interaction energies for a proton, thus simulating a protonic receptor site.[35–47] The MEP pattern for these products is similar and proton acceptor sites (where the potential is more negative) are generated by the oxygens of SO_2 and ureic carbonyl groups, together with the heterocyclic nitrogens (Figs 6, 7). These proton acceptors may therefore be considered as potential binding sites for ALS.

Table 4. Reactivity indexes [$R_{(i)\ HOMO}$] for compounds **1**–**8**

Compound	N-10	N-19	N-21	C-1	C-2	C-4	C-5	C-19	E_{HOMO} (eV)
1(A)	1.36	—	$2.49\times10-^{3}$	2.75×10^{-5}	1.58×10^{-6}	2.05×10^{-5}	8.71×10^{-5}	4.66	−9.306
1(B)	1.48	—	0.685	9.32×10^{-5}	4.03×10^{-5}	2.43×10^{-5}	8.20×10^{-5}	4.43	−9.556
1(C)	1.28	—	0.701	1.11×10^{-4}	8.0×10^{-6}	4.55×10^{-5}	4.05×10^{-5}	4.65	−9.376
1(D)	1.50	—	0.615	2.9×10^{-5}	1.37×10^{-4}	8.65×10^{-5}	3.02×10^{-4}	4.40	−9.594
1(E)	1.27	—	0.462	1.16×10^{-4}	1.41×10^{-4}	5.07×10^{-5}	3.95×10^{-5}	4.65	−9.391
2(A)	1.75	—	8.02×10^{-3}	9.35×10^{-4}	6.39×10^{-4}	1.54×10^{-5}	3.44×10^{-5}	4.03	−10.032
2(B)	1.61	—	0.822	2.0×10^{-6}	7.92×10^{-6}	9.25×10^{-5}	1.05×10^{-5}	4.22	−9.893
3(A)	2.27	2.28	2.75	1.29×10^{-4}	1.82×10^{-3}	9.54×10^{-5}	1.64×10^{-4}	–	−10.154
3(B)	2.14	2.26	2.75	1.15×10^{-4}	6.24×10^{-5}	6.48×10^{-5}	1.12×10^{-4}	–	−10.161
3(C)	2.75	1.88	2.49	2.48×10^{-2}	6.18×10^{-2}	2.23×10^{-2}	1.87×10^{-1}	—	−10.390
4(A)	1.27×10^{-3}	1.88×10^{-4}	1.97×10^{-4}	2.05	1.83	2.72	1.35	—	−10.074
5(A)	1.71	—	1.27	1.08×10^{-4}	2.79×10^{-5}	9.25×10^{-5}	8.26×10^{-5}	3.82	−9.684
6(A)	1.33	—	0.575	3.22×10^{-6}	8.83×10^{-6}	4.12×10^{-6}	1.99×10^{-5}	4.56	−9.392
6(B)	1.37	—	0.635	4.90×10^{-6}	1.46×10^{-5}	1.71×10^{-5}	3.24×10^{-5}	4.58	−9.392
6(C)	1.36	—	5.85×10^{-5}	4.14×10^{-6}	1.41×10^{-5}	1.93×10^{-5}	3.94×10^{-5}	4.59	−9.381
7(A)	9.9×10^{-5}	3.46×10^{-5}	3.15×10^{-5}	2.16	1.98	2.56	1.57	—	−10.018
7(B)	7.17×10^{-5}	1.78×10^{-5}	6.46×10^{-5}	2.16	1.96	2.55	1.58	—	−10.093
7(C)	7.86×10^{-5}	2.94×10^{-5}	9.55×10^{-5}	2.15	1.97	2.56	1.58	—	−10.083
8(A)	2.37	—	0.98	1.18×10^{-4}	0.783	8.31×10^{-5}	1.02×10^{-3}	3.44	−9.630
8(B)	2.24	—	0.86	7.93×10^{-5}	4.22×10^{-5}	2.43×10^{-5}	7.74×10^{-5}	3.67	−9.464
8(C)	2.42	—	0.95	1.16×10^{-4}	1.45×10^{-4}	9.9×10^{-5}	1.81×10^{-3}	3.55	−9.364

Table 5. IC_{50} for sulphonylureas **1**–**8**[15–17]

Sulphonylurea	IC_{50} (nM)
Primisulfuron®, **2**	5
Chlorimuron ethyl®, **5**	6
Rimsulfuron®, **6**	10
Sulfometuron methyl®, **8**	15
Bensulfuron methyl®, **1**	15
Metsulfuron methyl®, **3**	20
Chlorsulfuron®, **7**	21
Triasulfuron®, **4**	40

Conclusions

The results obtained confirm that sulphonylureas herbicide activity is strictly correlated with some of the most significant quantum descriptors of molecular electronic properties, such as the frontier m.o. distribution, charge density, HOMO and LUMO 3D shapes and MEP.[48] The experimental values of IC_{50} for sulphonylureas **1**–**8** are in good agreement with the values of these computed properties, since molecules with lower activity strongly differ from the general trend. Thus, the calculation, together with the analysis of these set of descriptors, can help to predict the activity of new molecules of this class of herbicides, since it can distinct between high, medium and low activity compounds. Following this approach, it will be possible to develop a 3D model for the active site of ALS, which could result useful for better understanding and predicting the activities of new herbicide compounds.

Molecular Orbital Quantum Calculations

Theoretical conformational analyses were performed by using the semi-empirical quantum mechanical AM1 method developed by Dewar.[21,22,49] The good performance of this method is well known in predicting the heat of formation and the MEP distribution and other more sophisticated methods such as ab initio quantum mechanical methods would have been rather time consuming.

The analysis of the conformational space was performed by varying all the degrees of freedom (i.e., torsional angles) by using the Monte Carlo[19] search as

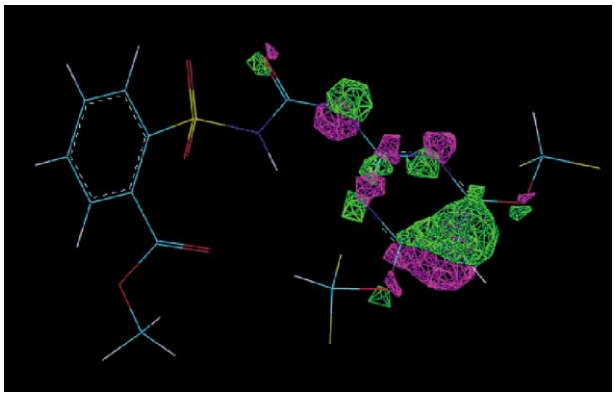

Figure 1. HOMO 3D shape for primisulfuron **2**.

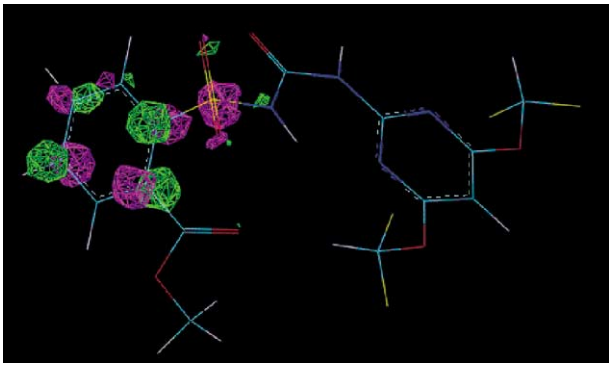

Figure 2. LUMO 3D shape for primisulfuron **2**.

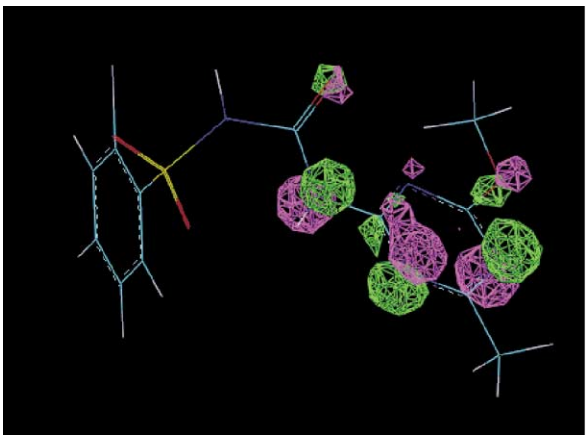

Figure 3. HOMO 3D shape for chlorsulfuron **7**.

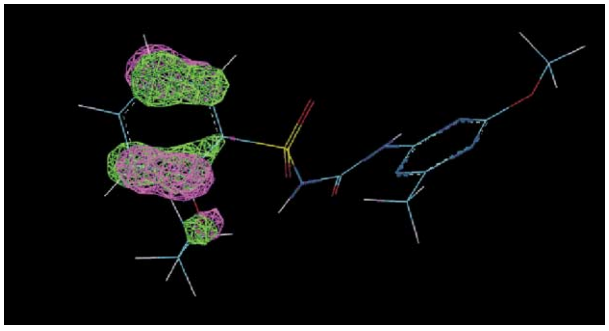

Figure 4. HOMO 3D shape for Triasulfuron **4**.

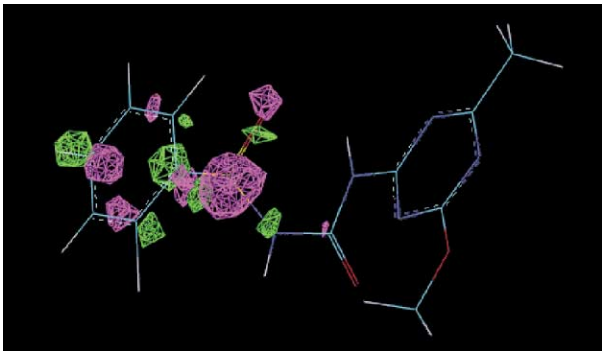

Figure 5. LUMO 3D shape for Chlorsulfuron **7**.

implemented in both the HyperChem 5.2/Chemplus 2.0 software package and HyperChem 4.6 (SGI-IRIX version).[49,50]

Atomic charges were calculated by Mulliken[23] charge population analysis. The stereoelectronic properties were calculated from the optimized geometry at AM1 level of the theory. The MEP maps for all molecules were generated beyond the molecular Van der Waals surface.[24]

The regions of positive electrostatic potential indicate excess positive charge (i.e., repulsion for the positively charged test probe), while regions of negative potential indicate areas of excess negative charge (i.e., attraction of the positively charged test probe) and this encoding

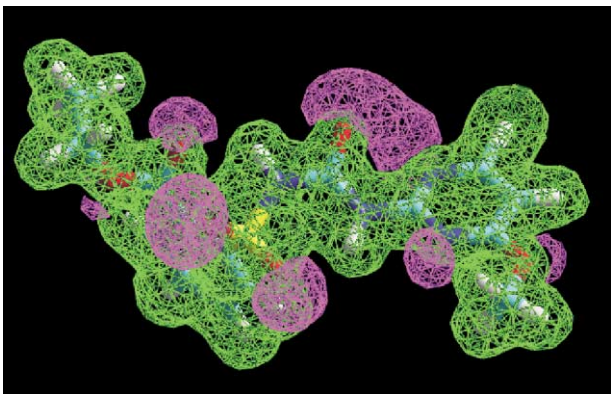

Figure 6. 3D visualisation of the molecular electronic potential (MEP) for sulphonylurea chlorimuron **5** beyond the Van der Waals surface based on AM1 wavefunction (approximately 1.5 Å away).

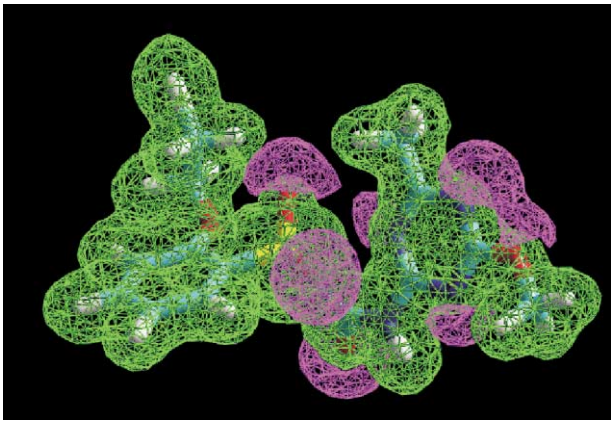

Figure 7. 3D visualisation of the molecular electronic potential (MEP) for sulphonylurea Triasulfuron **4** beyond the Van der Waals surface based on AM1 wavefunction (approximately 1.5 Å away).

was done by using colours. The most positive potential lies in the green regions, whereas the most negative potential lies in the pink ones (Figs 6, 7).

Acknowledgements

We thank C.N.R (Roma, Italy) and M.I.U.R. (Roma, Italy, PRIN 2000) for financial support.

References and Notes

1. Levitt, G. In *Pesticide Chemistry: Human Welfare and Environment*; Miymato, J.; Kearney, P. C, Eds.; Pergamon: New York, 1983; Vol. 1, p. 243.
2. Sauers, R. F., Levitt, G. In *Pesticide Synthesis Through Rational Approaches*; Magee, P. S., Kohn, G. K., Mean, J. J., Eds.; American Chemical Society: Washington, 1984; p 21.
3. Beyer, E. M.; Duffy, M. J.; Hay, J. V.; Schlueter, D. D. In *Sulphonylurea Herbicides in Herbicides: Chemistry, Degradation and Mode of Action Vol. 3*; Kearney, P. C., Kaufman, D. D., Eds.; Marcel Dekker: New York, 1988; Chapter 3, pp 117
4. Berger, B. M.; Wolfe, N. L. *Environm. Toxicol. Chem.* **1996**, *15*, 1500.

5. Shalaby, L. M.; Bramble, F. Q.Jr.; Lee, P. W. *J. Agric. Food Chem.* **1992**, *40*, 513.
6. Strek, H. J. *Pestic. Sci.* **1998**, *53*, 29.
7. Bray, L. D.; Heard, N. E.; Overman, M. C.; Vargo, J. D.; King, D. L.; Lawrence, L. J.; Phelps, A. W. *Pestic. Sci.* **1997**, *51*, 56.
8. Schneiders, G. E.; Koeppe, M. K.; Naidu, M. V.; Horne, P.; Brown, A. M.; Mucha, C. F. *J. Agric. Food Chem.* **1993**, *41*, 2404.
9. Marucchini, C.; Luigetti, R. *Pestic. Sci.* **1997**, *51*, 102.
10. Karelson, M.; Lobanov, V. S.; Katritsky, A. R. *Chem. Rev.* **1996**, *96*, 1027.
11. Franke, R. *Theoretical Drug Design Methods*; Elsevier: Amsterdam, 1984, p 115.
12. Zhou, Z.; Parr, R. G. *J. Am. Chem. Soc.* **1990**, *112*, 5720.
13. Osmialowski, K.; Halkiewicz, J.; Radecki, A.; Kaliszan, R. *J. Chromatogr.* **1985**, *346*, 53.
14. Nakayama, A.; Hagiwara, K.; Hashimoto, S.; Shimoda, S. *Quant. Struct. Act. Relat.* **1993**, *12*, 251.
15. Lu, R.; Yang, H.; Shang, Z.; Wang, W.; Pan, Y.; Zhao, X. *Science in China (Series B)* **1996**, *39*, 78.
16. Guttieri, M. J.; Eberlein, C. V.; Thill, D. *Weed Sci.* **1995**, *43*, 175.
17. Currie, R. S.; Kwon, C. S.; Penner, D. *Weed Sci.* **1995**, *43*, 578.
18. Mekki, M.; Leroux, G. D. *Weed Sci.* **1994**, *42*, 327.
19. Chang, G.; Guida, W. C.; Still, W. C. *J. Am. Chem. Soc.* **1989**, *111*, 4379.
20. (a) We chose as descriptors HOMO–LUMO energy gap, their topology, the frontier electron density (directly related to the measure of proton affinity), the heat of formation, the reactivity index, partial charges and MEPs because these are the most significant quantum chemistry descriptors to understanding the mechanism of binding with the enzyme, as it was already proved in studies of both other classes of ALS herbicides and other bioactive compounds. For significant examples, see: López-Romero, E.; Evrard, G.; Durant, F.; Sevrin, M.; George, P. *Bioorg. Med. Chem.* **1998**, *6*, 1745. (b) Werbovets, K. A.; Bhattacharjee, K. A.; Brendle, J. J.; Scovill, J. P. *Bioorg. Med. Chem.* **2000**, *8*, 1741. (c) Ref. 15. The heat of formation can be considered instead of total energy since the conformational analysis was carried out by using a semiempirical method since we could not use ab initio methods in order to calculate these properties. Eventually, the molecular volume and surface are still important, but especially in helping to choose the most active conformers of a compound and will be considered in a further study aimed to develop a receptor model of this class of herbicide.
21. Dewar, M. J. S.; Zoebish, E. G.; Healy, E. F.; Steward, J. J. P. *J. Am. Chem. Soc.* **1985**, *107*, 3902.
22. Dewar, M. J. S.; Dieter, K. M. *J. Am. Chem. Soc.* **1986**, *108*, 8075.
23. Mulliken, R. J. *Chem. Phys.* **1955**, *25*, 1833.
24. Pearson, R. G. *J. Org. Chem.* **1989**, *54*, 1423.
25. Burdett, J. K.; Coddens, B. A. *Inorg. Chem.* **1988**, *27*, 3259.
26. Faust, W. L. *Science* **1989**, *245*, 37.
27. Muetterties, E. L.; Beier, B. F. *Bull. Soc. Chim. Belg.* **1975**, *84*, 397.
28. Fukui, K. *Theory of Orientation and Stereoselection*; Springer: New York, 1975, p34.
29. Fleming, I. *Frontier Orbitals and Organic Chemical Reactions*; John Wiley & Sons: New York, 1976.
30. Tuppurainen, K.; Lotjonen, S.; Laatikainen, R.; Vartiainen, T.; Maran, U.; Strandberg, M.; Tamm, T. *Mutat. Res.* **1991**, *247*, 97.
31. Prabhakhar, Y. S. *Drug Des. Deliv.* **1991**, *7*, 227.
32. In order to measure the reactivity of HOMO orbital of atom *i*, the $R_{(i)}$ index is defined $R_{(i)} = f_{r(i)} / -E_{HOMO} \times 100$, where $f_{r(i)}$ = frontier electron density of HOMO at atom *i* E_{HOMO} = energy of the HOMO orbital (measured in eV) [the R(*i*) values are important for the herbicidal activity].
33. Naray-Szabo, G.; Ferenczy, G. G. *Chem. Rev.* **1995**, *95*, 829.
34. Bonaccorsi, R.; Scrocco, E.; Tomasi, J. *J. Chem. Phys.* **1970**, *52*, 5270.
35. (a) Politzer, P.; Thrular, D. G. *Chemical Applications of Atomic and Molecular Electrostatic Potential*; Plenum: New York, 1981. (b) Scrocco, E.; Tomasi, J. *Adv. Quantum Chem.* **1978**, *11*, 15.
36. Murray, J. S.; Politzer, P. *J. Mol. Struct. (Theochem.)* **1988**, *180*, 161.
37. Murray, J. S.; Politzer, P. *J. Mol. Struct. (Theochem.)* **1989**, *187*, 95.
38. Kikuki, O. *J. Mol. Struct. (Theochem.)* **1986**, *138*, 121.
39. Murray, J. S.; Politzer, P. *Theor. Chim. Acta* **1987**, *72*, 507.
40. Murray, J. S.; Evans, P.; Politzer, P. *Int. J. Quantum Chem.* **1990**, *37*, 271.
41. Pepe, G.; Siri, D.; Reboul, J. P. *J. Mol. Struct. (Theochem.)* **1992**, *256*, 175.
42. Guha, S. W.; Majumdar, D.; Bhattacharjee, A. K. *J. Mol. Struct. (Theochem.)* **1992**, *256*, 61.
43. Sheridan, R. P.; Allen, L. C. *J. Am. Chem. Soc.* **1981**, *103*, 1544.
44. Naray-Szabo, G. *Int. J. Quantum Chem.* **1982**, *22*, 575.
45. Naray-Szabo, G. *Int. J. Quantum Chem.* **1983**, *23*, 723.
46. Brasseur, J. L.; Dive, G.; Dehareng, D.; Ghuysen, J.-M. *J. Theor. Biol.* **1990**, *145*, 183.
47. Naray-Szabo, G. *Int. J. Quantum Chem.* **1979**, *16*, 265.
48. Neither a relationship or an equation (QSAR/QSPR) was included since the activity data belong to a number of sulphonylureas, which is not large enough to develop a significant equation.
49. HyperChem™ Software package version 4.5 e 5.02, Hypercube, Inc., Gainesville, FL, USA.
50. MacroModel V.5.5: Mohamadi, F.; Richards, N. G. J.; Guida, W. C.; Liskamo, R.; Lipton, M.; Caulfield, C.; Chang, G.; Hendrickson, T.; Still, W. C. *J. Comput. Chem.* **1990**, *11*, 440.